

5-2019

Thyroid Hormone Receptor and Coregulators: A Dynamic Model

Xiaopeng Sun

Follow this and additional works at: <https://scholarworks.wm.edu/honorsthesis>



Part of the [Cell Biology Commons](#), and the [Dynamic Systems Commons](#)

Recommended Citation

Sun, Xiaopeng, "Thyroid Hormone Receptor and Coregulators: A Dynamic Model" (2019). *Undergraduate Honors Theses*. Paper 1406.

<https://scholarworks.wm.edu/honorsthesis/1406>

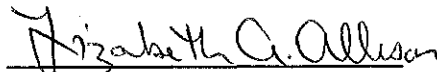
This Honors Thesis is brought to you for free and open access by the Theses, Dissertations, & Master Projects at W&M ScholarWorks. It has been accepted for inclusion in Undergraduate Honors Theses by an authorized administrator of W&M ScholarWorks. For more information, please contact scholarworks@wm.edu.

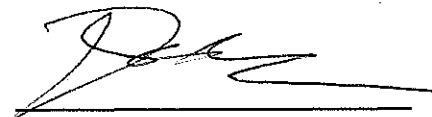
Thyroid Hormone Receptor and Coregulators: A Dynamic Model

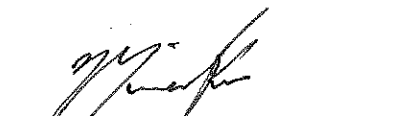
A thesis submitted in partial fulfillment of the requirement for the degree of Bachelor
of Science in CAMS Mathematical Biology with Honors in Biology From
The College of William and Mary in Virginia

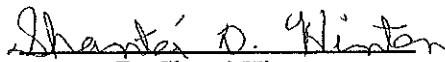
By
Xiaopeng Sun

Accepted for Honors


Dr. Elizabeth Allison (Advisor)


Dr. M. Drew LaMar


Dr. Mainak Patel


Dr. Shantá Hinton

Williamsburg, VA
2 May 2019

Abstract:

The thyroid hormone receptor (TR) mediates gene transcription in response to thyroid hormone (T3) and significantly affects cell growth, development and metabolism.

Although TR shuttles rapidly between the nucleus and cytoplasm, it is primarily nuclear localized at steady state. This state, according to previous research, is achieved by the balance of TR nuclear import, export and nuclear retention. The first focus of this thesis was on how nuclear receptor corepressor 1 (NCoR1) contributes to TR nuclear localization. Using transient transfection assays and fluorescence microscopy, we measured the fluorescent intensity of GFP or mCherry-tagged TR in the nucleus (N) and cytoplasm (C) of HeLa cells, and then calculated the N/C ratio as an indicator of intracellular localization patterns. We discovered that when NCoR1 is knocked down by shRNA, the amount of TR in the nucleus decreased significantly (lower N/C ratio). Inversely, when NCoR1 is over-expressed, the amount of TR in the nucleus significantly increased (higher N/C ratio). An even more dramatic cytosolic shift was observed for a TR mutant that cannot bind to NCoR1. Taken together, our results suggest that NCoR1 is a key regulator of TR nuclear retention. The second focus of this thesis was on developing a model to calculate protein-protein and protein-DNA binding rates using fluorescent recovery after photobleaching (FRAP). The model was designed to describe the fluorescent recovery curve for a linear photobleached region under a uniform laser profile. By fitting the model, we could then obtain binding rates for the complexes that interact with TR. These findings will contribute to the development of a dynamic mathematical model that aims to predict

TR's N/C ratio during the interaction with different complexes, and the effect of altered localization on transcriptional output of T3-dependent genes.

Table of Contents

List of Figures	1
Acknowledgements	2
Introduction	3-17
General Introduction.....	3
Thyroid Hormone	4
Thyroid Hormone Receptor.....	5
Nucleocytoplasmic shuttling	7
Intranuclear mobility and nuclear retention.....	8
Nuclear Receptor Corepressor.....	10
RNA interference.....	13
Fluorescence recovery after photobleaching (FRAP) and protein binding kinetics.....	14
Thesis Objective	18
Experimental Methods	19-25
Plasmids.....	19
Cell culture and transfection.....	19
Nucleocytoplasmic distribution analysis	20
NCoR1 shRNA knockdown validation	21
One dimensional line FRAP model	21
Results	26-36
Knock-down of NCoR1 promotes TR α 1 export.....	26
NCoR1 overexpression promotes TR α 1 nuclear localization	27
AHT-TR α 1 exhibits a significant cytosolic shift	28
The one dimensional FRAP model simulation.....	28
Discussion	37-42
Future Directions	43-46
Reference	47-50

Figures:

Figure 1: Structure of thyroid hormone receptor isoforms and AHT mutant

Figure 2: Structure of nuclear receptor corepressor and mechanism of ligand-dependent gene activation

Figure 3: NCoR1 knockdown leads to a TR α 1 cytosolic shift.

Figure 4: NCoR1 overexpression leads to enhanced TR α 1 nuclear localization.

Figure 5: AHT-TR α 1 is more cytosolically distributed compared to wild-type TR α 1

Figure 6: Simulated fluorescent recovery curve using different models

Figure 7: Graphic representation for TR localization model

Acknowledgements

I would like to express my deepest appreciation to my principal investigator Dr. Allison, who has been my mentor and guide when I developed my interest in science. With her support, I was able to forge my skills in biological research and find a direction that I am truly passionate about. I would like to thank our lab manager, Vincent Roggero, who not only keeps the lab well-maintained but also educated and trained me to perform successful experiments. Without their support, this research would not have been possible. I would also like to thank my committee members Dr. Shantá Hinton, Dr. Drew LaMar, and Dr. Mainak Patel for reviewing this work and their influence on my development as a student who has interests in interdisciplinary research.

I would like to offer my special thanks to Allison Lab members. We together form a supportive and inspiring community. During my time in the Allison Lab, our previous graduate students Cyril Anyetei-Anum and Matt Femia gave me much inspiration and guidance. Last but not least, my immense sense of gratitude goes to my parents, who always encourage me to pursue my dreams and support me without hesitation.

CHAPTER 1: INTRODUCTION

General Introduction:

The thyroid hormone receptor (TR) is a member of the nuclear receptor (NR) superfamily. It regulates cell metabolism, growth and development by serving as a ligand-dependent transcription factor. Since the discovery of its nucleocytoplasmic shuttling property in 2001 [Bunn et al., 2001], the lab has been focusing on the mechanisms that regulate TR intracellular localization. Currently, with various coregulatory complexes and nuclear shuttling pathways discovered, the TR localization network has become increasingly clear. This thesis had two major goals. The first goal was to examine the effect of nuclear receptor corepressor 1 (NCoR1) on TR nuclear localization using NCoR1 overexpression, knockdown of NCoR1, and a TR mutant that is defective for binding NCoR1. The second goal was to analyze existing fluorescence recovery after photobleaching (FRAP) data and derive TR-coregulator binding rates from the data. Results from this thesis research will eventually contribute to a mathematical model that could predict the amount of nuclear TR under normal and pathological conditions. Since gene regulation is a multifaceted process, understanding and predicting TR localization patterns will give us insight into developmental disorders and endocrine diseases.

Thyroid Hormone:

Thyroid hormone (TH) is an important ligand that regulates genes responsible for cell growth, development and metabolism. The production of TH is regulated by a feedback loop in the hypothalamic-pituitary-thyroid (HPT) axis [Yen, 2001; Yen et al., 2005]. After the thyroid gland receives the signal from the hypothalamus, it produces thyroxine (T₄), the most abundant type of TH the thyroid gland produces, and triiodothyronine (T₃), the active form of TH [Gnocchi et al.,2016]. Those two types of TH travel in the blood stream and enter target cells directly through facilitated transport. Besides interacting with TR after crossing the plasma membrane, it also has been discovered that a small proportion of TH interacts with the plasma membrane receptor $\alpha\beta 3$ to regulate gene expression [Davis et al.,2011].

T₃ and T₄ are structurally similar but T₄ contains an additional iodine. While T₄ is the thyroid gland's major product, it only indirectly participates in gene regulation through a cell signaling cascade. In order to directly mediate gene expression, T₄ is converted to T₃ rapidly by iodothyronine deiodinases in the target cells [Marsili et al.,2011]. T₃ then binds to TR to activate or repress target genes at sites known as thyroid hormone response elements (TREs). A TRE is a repeated sequence, TAAGGTCA, which is located in the regulatory regions of DNA [Kim et al.,1992]. Many NRs tend to be localized to the cytosol in the absence of ligand and only enter the nucleus after ligand interaction. For those NRs, ligand interaction is necessary for a conformational change that reveals the nuclear localization signal (NLS) [Vandevyver et al., 2012]. Different from those NRs, TR can bind to a TRE both

when ligand is absent and present. TR usually dimerizes with the retinoid X receptor (RXR), and then binds to a TRE. In the absence of T3, a TR dimer can repress gene transcription by forming corepressor complexes with NCoR1 and similar variants [Brent, 2012].

When T3 is present and binds TR, a conformational change occurs in TR, specifically at the helix 12 region located in the ligand binding domain [Wagner et al.,1995]. The conformational change reveals a surface that facilitates coactivator binding and detachment of corepressors. This structural change in TR ensures that it can only bind to one type of coregulatory factor, which facilitates the creation of a mathematical model that describes the binding rates. The complex interactions between TR and coregulators are critical for gene expression. Studying these relationships will greatly facilitate our understanding of TR function.

Thyroid hormone receptor:

Thyroid hormone receptors have alpha and beta subtypes encoded by *THRA* on chromosome 17q11, or *THRB* on chromosome 3q24, respectively [García-Silva et al., 2010]. Due to alternative splicing of the TR α and TR β mRNA transcripts, there exist various TR isoforms such as TR α 1, TR α 2, TR β 1, and TR β 2 [Selmi-Ruby and Rousset, 1996]. These isoforms serve various functions in different tissues and during different times of development. Most of the TR isoforms are known to be activated upon T3 binding and regulate cell development and metabolism; however, the function of TR α 2 and TR β 3 still remains mysterious [Jazdzewski et al., 2011]. This thesis focuses

on TR α 1 (Figure 1), which is one of the most abundant isoforms found in the human body.

The thyroid hormone receptor shares a similar structure with various nuclear receptors. It has an N-terminal transactivation domain that contains activation function-1(AF1), a DNA-binding domain, a hinge domain, a ligand-binding domain, and a C-terminal region that contains activation function-2 (AF2) [Zhang and Lazar, 2000]. The DNA-binding domain and ligand-binding domain are conserved throughout the TR isoforms, while the N- and C-terminal regions differ slightly. Therefore, such differences may be important for TR isoforms to exert different functions in different tissues [Selmi-Ruby et al., 1998]. Similar to the AF1 discovered in other nuclear receptors such as the estrogen receptor, TR's AF1 has transactivation function even when the ligand T3 is absent [Duma et al., 2006]. However, the function in general is weak until TR is fully activated and AF1 can synergize with AF2. The hinge domain of TR is where the primary nuclear localization signal (NLS-1) is located [Mavinakere et al., 2012]. Different from TR β 1, which only contains NLS-1 at the hinge region, TR α 1 also contains NLS-2 within the N-terminal transactivation domain. This difference in NLSs causes TR α 1 to be slightly more nuclear localized [Bunn et al., 2001; Baumann et al., 2001; Zhu et al., 1998]. The ligand-binding domain is critical for T3 binding, coregulator recruitment, and TR dimerization with RXR. The conformational change induced by T3 binding leads to corepressor release and coactivator recruitment. Then, the coactivator complex leads to corresponding gene

transcription. Due to the existence of AF1, it is also possible for TR to activate gene transcription when T3 is absent; however, the extent of such activation does not match the typical ligand binding activation [Duma et al.,2006].

Nucleocytoplasmic shuttling:

Since the discovery of TR's capability of nucleocytoplasmic shuttling [Bunn et al., 2001], there has been increasing attention on the mechanism of transport and factors that could restrict TR's intracellular mobility. Currently, we know that TR is transported between the nucleus and cytoplasm through the nuclear pore complexes (NPCs), structures consisting of nucleoporins that reside on the nuclear membrane [Pemberton and Paschal, 2005]. Usually, the pore complex has a diameter of 50 nm. Molecules that are smaller than 50 kDa can passively diffuse through the NPC or enter the nucleus by facilitated transport. For macromolecules such as TR, however, they must pass through the pore complex by binding with transport proteins called karyopherins. Karyopherins are known to recognize and dock to the phenylalanine-glycine rich region in the NPC and carry the cargo across the nuclear envelope.

The karyopherins that recognize TR's NLSs are importin 7, importin β 1 and the adapter importin α 1 [Roggero et al., 2016]. Importin 7 only interacts with NLS-2 that explicitly belongs to TR α 1, causing it to be more nuclear localized compared to other TR subtypes. Exportins 4, 5, and 7 [Subramanian et al., 2015] are known to recognize TR's nuclear export signals (NESs) in helix-3, helix-6, and helix-12 of the ligand-binding domain and shuttle TR to the cytoplasm [Mavinakere et al., 2012].

From structural studies of importins and exportins, it is understood that there exists flexibility in their shape which allows interaction with various cargos [Sorokin et al., 2007]. The nuclear import and export pathways are regulated by the Ran-GTP/GDP cycle. Importin $\alpha 1$ first binds to the NLS of the cargo, and importin $\beta 1$ interacts with the phenylalanine-glycine repeats of the NPC [Gorlich et al., 1995; Hoelz et al., 2011; Suntharalingam and Wenthe, 2003]. Then, the heterodimeric complex shuttles the cargo into the nucleus. In the nucleoplasm, Ran-GTP binds to the importin and causes the release of cargo [Gorlich et al., 1996]. In the nucleus, Ran-GTP facilitates binding between exportins and cargo and shuttles the complex to the cytoplasm [Pemberton and Paschal, 2005; Sorokin et al., 2007]. When Ran-GTP passes through the cytoplasmic filaments around the NPC, it is hydrolyzed to Ran-GDP, which then causes the release of the cargo [Pemberton and Paschal, 2005].

Intranuclear mobility and nuclear retention:

Although the movement of some macromolecules, protein aggregates, and protein-containing vesicles of the secretory system, is facilitated by motor proteins on the cytoskeleton [Brangwynne et al., 2008], the model described in this thesis is based on the common assumption that proteins in the cytosol and nucleoplasm undergo Brownian motion. We also assumed that the cytosol and nucleoplasm are low Reynolds number liquids, which means that a liquid's movement is dominated by viscous forces and the movement is smooth and constant. Compared to proteins diffusing in diluted buffer solution, proteins studied *in vivo* tend to experience a decrease in diffusion rate due to overcrowding of the cellular environment and

potential interaction with other proteins [Roosen-Runge et al., 2011]. Therefore, before any model creation, it is important to remember that the assumptions made about viscosity of the nucleoplasm and cytosol might be inaccurate. One component that significantly affects diffusion rate, according to Einstein's model of Brownian motion in a low Reynolds number liquid, is the hydrodynamic radius of the protein [Einstein, 1905]. Therefore, as TR binds with other factors, such as importins, exportins, or coregulators, the complex's diffusion rate will dramatically change. Also, when TRs are actively involved in gene regulation, they will interact with DNA and become completely immobile, albeit only transiently. Based on the free diffusion assumption, protein-protein interactions and DNA-protein interactions are the two major aspects that could affect TR mobility and ultimately its localization.

Femia et al. [submitted 2019] and Baumann et al. [2001] demonstrated that coregulatory factors, already known to be indispensable for TR-regulated transcription activity, are also important for TR's intracellular distribution and mobility. One of the major aims of this thesis was to discover which coregulators affect TR localization so that we can eventually model the entire system mathematically. The research of Baumann et al. [2001] used a TR mutant that is defective in binding nuclear receptor corepressor1 (NCoR1) to provide evidence that NCoR1 contributes to TR nuclear retention. We now understand the structure of TR better, however, and the mutation selected in Baumann et al.'s research, given its localization near NLS-1, could lead to an undesired conformational change and potentially affect TR's binding with other coregulators, importins, and exportins.

Baumann et al. [2001] also indicated that the TR mutant's inability to interact with NCoR1 could be explained, in part, by its inability to remain in the nucleus where NCoR1 is localized. Therefore, their study remains inconclusive and the role of the NCoR1-TR interaction in nuclear retention requires further analysis.

Nuclear receptor corepressor 1:

The discovery of TR's capability to repress target gene expression in the absence of T3 immediately leads to questions about what molecular mechanism achieves such transcriptional silencing. The original hypothesis was that the mechanism involved interaction with basal transcription factors, such as the transcription factor II B (TFIIB), eventually inhibiting the formation of the preinitiation complex. This hypothesis, however, was soon disproved by further data which indicated that TR's C-terminal region, which interacts with TFIIB, is not sufficient for silencing [Horlein et al., 1995]. The data also indicated that a region in the hinge domain and part of the ligand-binding domain are required for gene silencing. This finding implies the existence of an additional interacting complex. Later, Horlein et al. [1995] discovered a 270 kDa protein that binds specifically to TR's hinge domain and ligand-binding domain in the absence of T3. Specific TR mutations that interrupt binding to this protein also eliminate ligand-independent gene repression. Taken together, data suggested that this protein, later known as NCoR1, mediated transcriptional silencing.

After the discovery of NCoR1, a similar corepressor, NCoR2 (originally called SMRT), was discovered. The complete crystal structures of NCoR1 and its homolog

are still not clear; however, through studying their interaction with TR and retinoic acid receptor, a few functional domains have been identified. In NCoR1, there exist LXXI/HIXXXI/L sequences that recognize and bind to target NRs. This sequence is similar to the LXXLL sequence in coactivators [Perissi et al., 1999; Nagy et al., 1999]. Based on the general agreement in sequence, corepressors and coactivators have been proposed to interact with lysine residues in helix 3 and glutamine residues in helix 12 in TR [Yen, 2001]. The slight difference in the length of the coregulators' interaction domain and the conformational change caused by ligand binding were once thought to be the factors that regulate the binding of coregulators [Perissi et al., 1999]. Currently, a dynamic stabilization model is proposed to explain the selective binding. In this model, helix 12 of TR is thought to be dynamic and can be eventually stabilized upon ligand binding so that it could interact with coactivators. The model also showed that ligand binding could stabilize the overall receptor structure to further facilitate transcription. Those two factors combined facilitate the binding of coactivators and release of corepressor [Pission et al., 2000; Johnson et al., 2000; Weikum et al., 2018].

NCoR1 also contains a major deacetylase activation domain and three repression domains [Figure 2a]. The major deacetylase activation domain (DAD) resides between P412-P480. The interaction between NCoR1 and a chromatin modification complex was first discovered by a group of researchers who used coimmunoprecipitation assays to observe the relationship between NCoR1 and histone deacetylase (HDAC) activity and discovered an overlap between the two [Heinzel et al., 1997]. There are

five HDAC isoforms, HDAC1, 7, 4, 3 and Sirt1, known to interact with NCoR1. Later it was confirmed that the HDAC3-NCoR1 interaction is essential for TR regulation. Those discoveries support the hypothesis that the TR/NCoR1 silencing complex uses histone deacetylation to condense the local chromatin, turning transcription off [Yen, 2001]. When T3 is added to the system, the repression is removed, coactivators are attached to TR and the chromatin is subsequently remodeled to initiate gene transcription (Figure 2b). These studies together demonstrated another method by which NCoR1 could silence gene expression. Currently, the functions of all repression domains are still under study. NCoR1 is known to recruit G protein pathway receptor 2 (GPR2) and transducing β -like protein 1 (TBL1). The three proteins then form a stable three ways complex that significantly enhances the function of HDAC3, which binds at the DAD motif [Oberoi et al.,2011]. The entire complex is known to facilitate HDAC3 interaction with inositol phosphates, critical elements for histone deacetylation [Watson et al., 2012]. NCoR1 is also known to bind with Class IIa HDACs. Instead of interacting with the DAD domain, HDAC4 and 5 are known to bind with repression domain 3 in NCoR1 [Fischle et al., 2002; Hudson et al., 2015]. This discovery further increases the complexity of NCoR1 regulated transcription silencing.

Previous research has found that NCoR1 interacts with TFIIB and two TATA binding protein associated factors [Yen,2001]. Thus, it is likely that NCoR1 at a negative TRE affects the recruitment of basal transcription factors. Makowski et al. [2003] discovered an NCoR1 homolog that had lost the repression domain. Surprisingly, this

truncated NCoR1 not only loses its ligand independent inhibition capability on a TRE, but also stops ligand dependent activation of a TRE when T3 is present. This interesting discovery reveals the importance of NCoR1 release in TRE activation.

As previously mentioned, Baumann et al. [2000] used a green fluorescent protein (GFP)-tagged mutant TR with a NCoR1 binding region mutation, called GFP-AHT-TR, to show that NCoR1 affects TR intracellular distribution. The TR β amino acid residues at positions 223-alanine, 224-histidine, and 227-threonine in the NCoR1 binding box were substituted to glycine, glycine, and alanine, respectively (AHT to GGA). Because the NCoR1 binding box is highly conserved between TR isoforms, the same substitutions were made at positions 174, 175, and 178 for TR α [Figure 1]. After transfecting cells with GFP-AHT-TR, a significant cytosolic shift was discovered by Baumann et al. [2001]. From this result, they concluded that another function of NCoR1 is to retain TR in the nucleus when T3 is absent. From the observation of different TR mutants discovered in cancer or developmental disorders, it is also clear that the balance between nuclear export, import and retention is critical for normal cell function [Zhang et al., 2017]. However, the exact mechanism between this balance and gene transcription remains unclear. After careful examination of the AHT mutant used in Baumann et al.'s study, there exists the possibility that the AHT mutant could affect TR's binding with factors other than NCoR1, such as importins. Therefore, one major goal of this thesis was to study the TR-NCoR1 interaction through overexpression and shRNA-mediated knockdown. If NCoR1 does contribute to nuclear retention, we predicted that we would observe a significantly greater

nuclear localization of TR when NCoR1 was overexpressed, if NCoR1 is not saturated in the system; and that we would observe a significant cytosolic shift of TR in the NCoR1 knockdown group.

RNA Interference:

RNA interference is a biological process that silences expression of a target gene by inactivating its messenger RNA (mRNA) product. mRNA inactivation is commonly achieved through either exogenous small interfering RNA (siRNA) and short hairpin RNA (shRNA) mediated RNA degradation, or endogenous microRNA induced translational suppression [Fire et al., 1998]. In this thesis, shRNA was used to achieve NCoR1 knock down. Compared to siRNA, shRNA has similar paired antisense and sense strands, but it also contains unpaired RNA that eventually forms a loop that connects and stabilizes the double stranded RNA. This structure grants shRNA a low degradation rate in the cell. After a shRNA plasmid is introduced into the target cell, it is transcribed by RNA polymerase. The product, pre-microRNA, is processed by Drosha protein and exported from the nucleus by exportin 5 [Elbashir,2001]. In the cytoplasm, the precursor is further processed by Dicer and TAR-RNA-binding protein, where the shRNA hairpin is removed. The processed shRNA is then loaded into the RNA-induced Silencing Complex (RISC). In the complex, the original sense strand is degraded, and the antisense strand recognizes the target mRNA by complementary base pairing. The RISC can then cleave the mRNA sugar-phosphate backbone to affect translation [Maniataki et al., 2005; Moore et al.,2010]

Fluorescence recovery after photobleaching (FRAP) and protein binding

kinetics:

Many interactions that take place in the cell can be described as a binding-diffusion process. As previously mentioned, the two major processes that contribute to TR nuclear retention, protein-protein interactions and DNA-protein interactions, can also be described using this method. Fluorescence recovery after photobleaching (FRAP) is one of the common methods for studying protein mobility and the reaction diffusion process in the cell. The target molecules studied in this thesis first were tagged with green fluorescent protein (GFP) to allow visualization. During FRAP, in a defined region of interest (ROI), confocal lasers in the microscope are used to rapidly and irreversibly photobleach the fluorescent fusion protein. The photobleached molecules will diffuse and exchange with the surrounding molecules over time. As the bleached and unbleached molecules mix in the ROI, an increase in the fluorescence levels at the photobleached region is obtained. The fluorescent intensity measurement of ROI overtime yields a recovery curve that contains information about the kinetic constants of the fluorescent tagged molecule, and its mobile and immobile fractions.

As FRAP has transformed from only focusing on lateral diffusion at the plasma membrane to basically all fluorescent fusion proteins, the kinetic analysis that can be conducted using the recovery curve is also evolving; however, researchers are still far from reaching a general agreement on the best analysis and experimental method to obtain a robust protein diffusion rate and binding rate [Seiffert and Oppermann, 2005;

Kang et al., 2010]. One commonly applied FRAP method uses a circular bleach region and calculates diffusion, as well as the binding rate using partial differential equations. Previous research in the Allison lab used a linear bleach region (called strip-FRAP) to accommodate the rapid diffusion kinetics of TR [Femia et al., and Anyetei-Anum et al., submitted 2019]. Therefore, developing a new equation for the diffusion rate and binding rate calculation, specifically for a linear bleach region, became the other goal of this thesis. Conveniently, we could still apply most of the partial differential equation derivation in Aifantis and Hill [1980] and the FRAP equation in Kang et al. [2008] to develop a FRAP equation that describes the fluorescent recovery curve of our linear photobleached region.

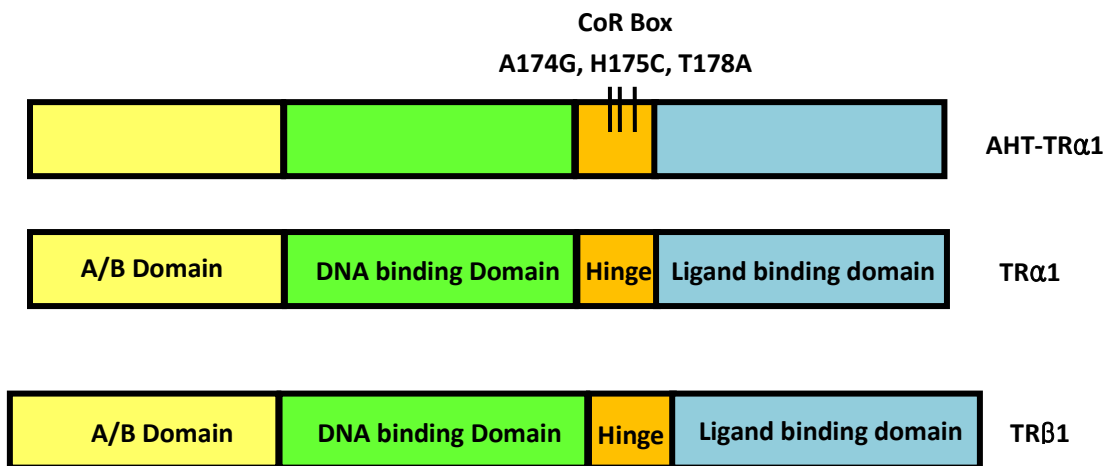


Figure 1: The structures of thyroid hormone receptor subtypes were adapted from Mavinakereet al.[2012], and the AHT-TR mutant comes from Horlein et al.[1995]. Comparatively, TR β 1 has a longer A/B domain while the rest of the domains remain highly similar. The mutations in AHT-TR α 1 are located in the hinge domain, a region that is conserved over TR isoforms that interact with corepressors.

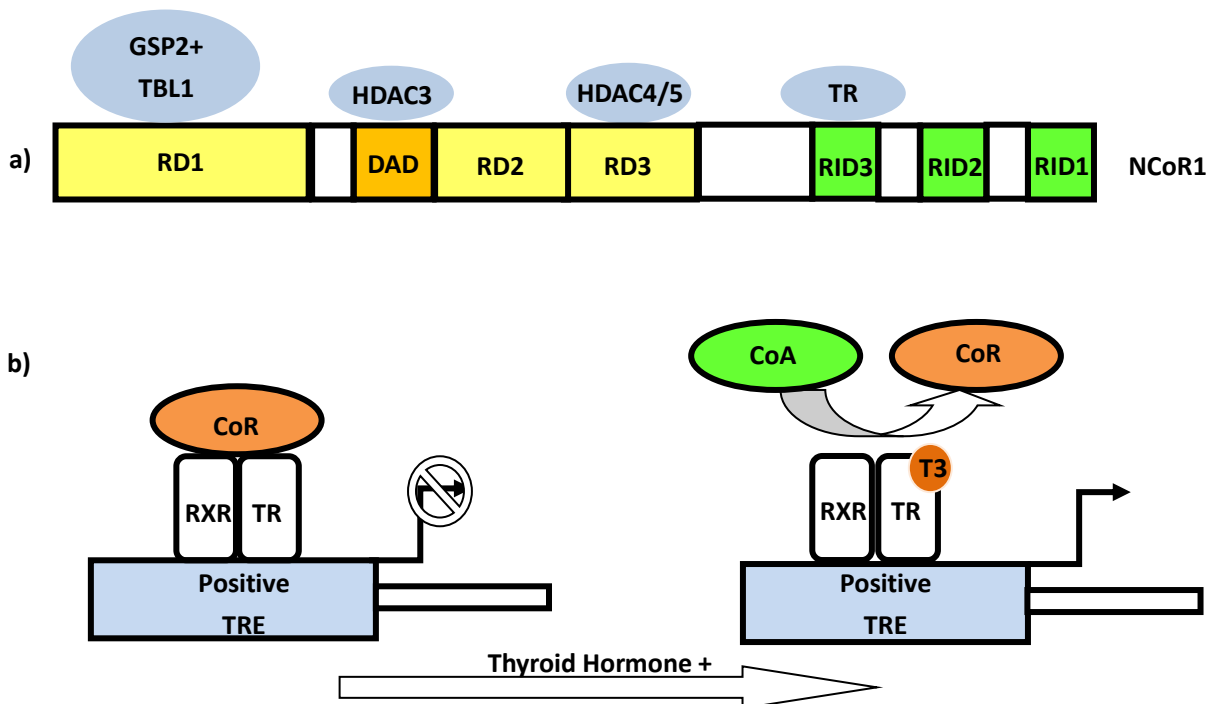


Figure 2: (a) NCoR1 contains three repression domains (RD1-RD3) and a deacetylase binding domain (DAD). It is known that GSP2 and TBL1 bind at RD1 and interact with HDAC3 to activate deacetylation. HDAC4 and 5 function independently and enhance the repression. RID3 in NCoR1 binds to TR while the other two interaction domains bind to other nuclear receptors. (b) In the absence of T3, NCoR1 (CoR) binds to the TR-RXR dimer and represses gene transcription at a positive TRE. When ligand is added, the helix 12 structure stabilizes to facilitate NCoR1 and coactivator (CoA) recruitment to initiate gene transcription.

Thesis Objective:

The balance of TR export, import, and nuclear retention is critical for proper gene silencing and activation [Mavinakere et al., 2012]. Therefore, an ordinary-differential-equations model that analyzes this dynamic system could bring insight to the behavior of TR and how disturbance could affect the system's stability. Before a TR localization model can be created and analyzed, however, there are two obstacles that need to be overcome. First, not all of TR's binding partners and coregulators have been identified, especially those that affect TR localization. Second, the binding rates between TR and other coregulators remain unclear. This thesis research targets those obstacles through two specific aims:

- 1) Evaluate whether overexpression and knockdown of NCoR1 alters nuclear retention of wild-type TR. Previously, Baumann et al. [2000] used the AHT-TR mutant to demonstrate that NCoR1 contributes to TR nuclear retention; however, how the structure of this mutant affects its NESs, NLSs, and binding with other coregulators remains unknown.
- 2) Develop a mathematical model that calculates protein-protein and protein-DNA binding rates from linear FRAP.

The results from this research will increase our understanding of TR's nuclear retention and provide parameters important for the TR localization model.

CHAPTER 2: EXPERIMENTAL METHODS

Plasmids: The EGFP and mCherry expression vectors were obtained from Clontech Laboratories. The GFP-NCoR1 plasmid was made by GenScript. mCherry-TR and GFP-TR wild-type plasmids were previously prepared [Bunn et al., 2001; Femia et al., submitted 2019]. The cDNA for AHT-TR was designed using GeneArt™ gene synthesis services, and subcloned into the EGFP expression vector by Vinny Roggero. Predesigned SureSilencing™ shRNA plasmid sets, consisting of four different shRNA expression plasmids for the target NCoR1 mRNA, were purchased from SABioscience, along with a scrambled sequence negative control.

Cell culture and transfection: HeLa cells were cultured in Minimum Essential Medium (MEM) supplemented with 10% fetal bovine serum (FBS) at 37 °C under 5% CO₂ and 98% humidity. All cells were grown to approximately 80% confluency before seeding into six-well culture dishes. When the optimal confluency was reached, cells were displaced with 0.25% trypsin (Gibco). Six-well culture dishes with 22mm Coverslips for Cell Growth (Fisher Scientific) were seeded with HeLa (human) cells at a density of 2.5×10^5 cells per well. Seeded cells were incubated for ~24 hours. Plates were then transfected or cotransfected with: (1) 2μg of GFP-TRα1, (2) 2μg of mCherry-TRα1, (3) 2μg of GFP-TRα1+2μg of NCoR1 shRNA, (4) 2μg of GFP-TRα1+2μg of NCoR1 shRNA, (5) 2μg of mCherry-TRα1+4μg of GFP-NCoR1, or (6) 2μg of GFP-AHT-TRα1. All transfections were facilitated by Lipofectamine 2000(Invitrogen) in Opti-MEM 1 reduced serum medium (Invitrogen), except for TR-NCoR1 co-transfection, which was facilitated by Lipofectamine 3000

(Invitrogen) in Opti-MEM 1. Reagents were used according to the manufacturer's protocol.

Nucleocytoplasmic distribution analysis: For Lipofectamine 2000 transfection, transfection mixtures were replaced with 10% FBS-MEM medium after 8 hours of transfection. For Lipofectamine 3000, the mixtures were replaced after 18-20 hours. After 24 hours of transfection with Lipofectamine 2000 (20-22 hours for Lipofectamine 3000), cells were washed with 1x Dulbecco's phosphate-buffered saline (DPBS) and fixed in 3.7% formaldehyde. Coverslips were mounted with Fluoro-Gel II mounting medium containing DNA DAPI stain onto a glass slide. The slide was visualized using a Nikon Plan Apo 40x/0.95 objective on the Nikon ECLIPSE TE 2000-E fluorescence microscope for quantitative analysis. The microscope facilitates fluorescence emission with the following filters: Nikon Ultraviolet Excitation via UV-2E/C filter (for DAPI visualization); Blue Excitation via B-2E/C filter (for GFP visualization); Red Excitation via T-2E/C filter (for mCherry visualization). Image capture and analysis were achieved by the HQ2 CCD camera (Photometrics, Tucson, AZ) and NIS-Elements AR software.

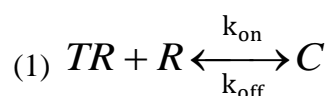
Prior to quantitative analysis, slides were blinded to ensure scoring was unbiased.

Region of interest (ROI) squares were placed in the nucleus and cytoplasm to measure the fluorescent intensity. The data for each measurement was exported to EXCEL. All experiments consisted of at least 3 biologically independent replicates and at least 100 cells in each replicate. Due to the low transfection rate in the TR-NCoR cotransfection

treatment, 10 replicates were performed with 30 cells scored in each replicate. The data were first tested for normality, then a student's T-test, or its non-parametric counterpart, Mann-Whitney-Wilcoxon Test, was used to calculate p-values and determine significance.

NCoR1 shRNA knockdown validation: HeLa cells were seeded at 8×10^5 cells per 100 mm dish. After 24 hours of incubation, the plate was transfected with 10 μ g NCoR1 shRNA with transfection facilitated by Lipofectamine 2000 in Opti-MEM1 medium. Transfection mixtures were replaced with 10%FBS-MEM medium after 8 hours of transfection. The HeLa cells lysates were prepared 16 hours after medium replacement. Protein concentration of the lysates was measured using NanoDrop amino acid measurement (ND-1000 Spectrophotometer) and 40 μ g of protein was loaded in each lane. Then, a western blot was performed using the primary antibody anti-NCoR1, 1:500; and secondary antibody anti-rabbit IgG, 1:50000. (The secondary antibody concentration was halved from standard lab protocol to decrease overexposure). Protein size was confirmed using Pre-Stained Kaleidoscope Protein Standards (Bio-Rad, Hercules, CA). Semi-quantification was used to determine band density.

One dimensional line FRAP model: We assumed a system of two reactants and their product. The general formula for TR coregulator binding can be described in a formula:



where TR represents thyroid hormone receptor, R represents coregulators, and C represents the binding complex. For the reaction kinetics, k_{on} is the binding rate and k_{off} is the disassociation rate. To convert (1) to a partial differential equation(PDE), we made the following assumptions: 1) because the linear bleach region bridges the nucleus, the exchange between fluorescent molecules and bleached molecules only happens in one dimension, the x axis; 2) the molecules participating in the reaction are under Brownian motion; 3) the ROI is small enough so that the entire nucleus can be regarded as infinitely large; and 4) the amount of coregulators is large so that the binding rate can be described as a pseudo-constant: $k_{on}^* = k_{on}R$. Therefore, we can reduce the equation describing R and write a system of first order PDEs:

$$(2) \quad \begin{aligned} \frac{\partial TR}{\partial t} &= D_{TR} \left(\frac{\partial^2 TR}{\partial x^2} \right) - k_{on}^* TR + k_{off} C \\ \frac{\partial C}{\partial t} &= D_C \left(\frac{\partial^2 C}{\partial x^2} \right) + k_{on}^* TR - k_{off} C \end{aligned}$$

Eventually, we can replace k_{on}^* with k_{on} for simplicity. This equation can also describe protein-DNA interaction when we set $D_C = 0$. The initial condition of the PDE system is:

$$C(x,0) = C_i \delta(x) \quad TR(x,0) = TR_i \delta(x)$$

where x represents the relative coordinate on the one-dimensional diffusion axis, and x=0 is the center of the bleach region. The Dirac delta function, which is represented as $\delta(x)$ in the initial condition, will assume bleached molecules are all located at position x=0 and nowhere else. The function $L(x)$, which we will use later for fluorescent intensity calculation, represents laser intensity profile and c is a laser constant. For this thesis, we chose a uniform laser profile where:

$$\begin{cases} L(x) = \frac{L_0}{r}, |x| \leq r \\ 0, |x| > r \end{cases}$$

L_0 is the initial laser intensity and r is half of the laser's width. Equation 2, with the initial conditions described above, has already been solved by Aifantis and Hill [1980] using Laplace transformation. Therefore, we can directly apply the one-dimensional version of the equation. The analytical solution is:

$$\begin{aligned} TR(x, t) &= \beta_1 e^{-t} \phi(x, t) + \\ &\frac{e^{\lambda t} \sqrt{K}}{1-D} \int_{Dt}^t e^{-\mu s} \phi(x, s) (\beta_1 \sqrt{\frac{s-Dt}{t-s}} I_1(\eta) + \beta_2 \sqrt{K} I_0(\eta)) ds \\ (3) \quad C(x, t) &= \beta_1 e^{-Kt} \phi(x, Dt) + \\ &\frac{e^{\lambda t} \sqrt{K}}{1-D} \int_{Dt}^t e^{-\mu s} \phi(x, s) (\beta_2 / \sqrt{\frac{s-Dt}{t-s}} I_1(\eta) + \beta_1 \frac{1}{\sqrt{K}} I_0(\eta)) ds \end{aligned}$$

Where:

$$\begin{aligned} D &= \frac{D_c}{D_{TR}}, K = \frac{k_{on}}{k_{off}} \\ \beta_1 &= \sqrt{\frac{k_{on}}{D_{TR}}} TR_i \\ \beta_2 &= \sqrt{\frac{k_{on}}{D_{TR}}} C_i \\ \lambda &= \frac{D+K}{1-D} \\ \mu &= \frac{1+K}{1-D} \\ \eta &= \frac{2\sqrt{K}}{1-D} \sqrt{(t-s)(s-Dt)} \\ \phi(x, Dt) &= \frac{1}{\sqrt{4\pi Dt}} e^{-\frac{x^2}{4Dt}} \end{aligned}$$

$I_1(\eta)$ and $I_0(\eta)$ stands for the modified Bessel function. According to Axelrod et al. [1976], we can convert the quantity of fluorescent molecules in Equation (3) to

fluorescent intensity using integrals and several properties of fluorescent emission

[Axelrod et al., 1976]. The FRAP formula thus is:

$$(4) \quad \begin{cases} F_{TR} = q\varepsilon \int_0^r L(x)TR(x,t)dx \\ F_C = q\varepsilon \int_0^r L(x)C(x,t)dx \\ F_{total} = F_{initial} - 2(F_{TR} + F_C) \end{cases}$$

The first two equations represent the diffusion bleached molecule and the third equation captures the recovery. Parameter q is the quantum efficiencies of light absorption, emission, and detection; and ε is the attenuation factor of the excitation laser beam. The relationship between those two parameters and the fluorescent intensity is: $F_{initial} = L_0 C_i q \varepsilon$

By plugging Equation (3) in (4), we found that we only needed to integrate the function that contains x , which is the diffusion equation. Thus, we first calculate the integration of ϕ :

$$\begin{cases} \int_0^r \phi(x,t)dx = \frac{1}{\sqrt{4\pi t}} \int_0^r e^{-\frac{x^2}{4t}} dx = \frac{1}{\sqrt{4\pi t}} \frac{1}{2} \sqrt{4\pi t} \times \text{erf}\left(\frac{r}{\sqrt{4t}}\right) = \frac{1}{2} \text{erf}\left(\frac{r}{\sqrt{4t}}\right) \\ \int_0^r \phi(x,Dt)dx = \frac{1}{\sqrt{4\pi Dt}} \int_0^r e^{-\frac{x^2}{4Dt}} dx = \frac{1}{\sqrt{4\pi Dt}} \frac{1}{2} \sqrt{4\pi Dt} \times \text{erf}\left(\frac{r}{\sqrt{4Dt}}\right) = \frac{1}{2} \text{erf}\left(\frac{r}{\sqrt{4Dt}}\right) \end{cases}$$

Finally, we can use this result in the FRAP equation and obtain:

$$\begin{aligned}
F_{TR}(t) &= \frac{q\epsilon L_0 \beta_1 e^{-t}}{2r} \operatorname{erf}\left(\frac{r}{4t}\right) + \\
&\frac{q\epsilon L_0}{2r} \frac{e^{\lambda t} \sqrt{K}}{1-D} \int_{Dt}^t e^{-\mu s} \operatorname{erf}\left(\frac{r}{\sqrt{4Ds}}\right) \beta_1 \sqrt{\frac{s-Dt}{t-s}} I_1(\eta) + \beta_2 \sqrt{K} I_0(\eta) ds \\
F_C(t) &= \frac{q\epsilon L_0 \beta_1 e^{-t}}{2r} \operatorname{erf}\left(\frac{r}{\sqrt{4Dt}}\right) + \\
&\frac{q\epsilon L_0}{2r} \frac{e^{\lambda t} \sqrt{K}}{1-D} \int_{Dt}^t e^{-\mu s} \operatorname{erf}\left(\frac{r}{\sqrt{4Ds}}\right) (\beta_2 / \sqrt{\frac{s-Dt}{t-s}} I_1(\eta) + \beta_1 \frac{1}{\sqrt{K}} I_0(\eta)) ds \\
F_{total}(t) &= F_{initial} - 2(F_{TR}(t) + F_C(t))
\end{aligned}$$

Matlab can then solve the integration numerically when we provide initial values for diffusion rate and binding constant. Then, we can compare the simulation result with FRAP data to obtain the appropriate parameter for the reaction using least square fit.

One advantage of this new equation, compared to the equation describing DNA-protein binding [Sprague et al., 2004], is that the new model does not need to assume the binding complex is immobile, making it suitable for studying the NR-coregulator interaction during overexpression.

CHAPTER 3: RESULTS

Knockdown of NCoR1 promotes TR α 1 export:

Although TR is known to shuttle rapidly between the nucleus and cytoplasm [Bunn et al., 2001], its nuclear localization pattern indicates the presence of factors that retain TR in the nucleus. In the absence of T3, NCoR1 binds with a TR-RXR heterodimer and anchors it at the TRE of a T3-responsive gene. Therefore, we hypothesized that NCoR1 could help retain TR in the nucleus and avoid nuclear export. From studying a TR mutant with a defective NCoR1 binding box, previous research suggested that NCoR1 and its isoforms could play a key role in TR nuclear retention [Baumann et al., 2001]. However, due to the potential effect this mutant has on TR-importin and TR-coactivator binding, the TR-NCoR1 interaction needed to be further studied. This thesis research examined the TR-NCoR1 interaction through altering NCoR1 concentration in the cell by shRNA-mediated knockdown of NCoR1.

First, we used western blot to confirm shRNA knockdown of NCoR1 in HeLa cells. We observed a marked decrease in the amount of NCoR1 in lysates from cells treated with NCoR1 shRNA compared with lysates from cells treated with the control shRNA (Figure 3a). However, precise quantification was not possible because the molecular weight of NCoR1 (270 kDa) required running the protein gel for an extended period. At the time the 250 kDa protein molecular weight standard reached the position of optimal separation, the 30kDa β -tubulin used as an internal control had run off the end of the gel.

After transfecting HeLa cells with GFP-TR expression plasmids and different quantities of NCoR1 shRNA, the nucleocytoplasmic distribution of TR was quantified. There was a significantly greater cytoplasmic population in the knockdown group (average N/C = 3.5 for 2 μ g shRNA and 2.8 for 4 μ g shRNA) compared to the control group (average N/C = 5.6) ($p < 0.01$). We also observed an increase in the cytoplasmic population as the shRNA concentration increased (Figure 3b). This result suggested that as the concentration of NCoR1 decreases, nuclear retention of TR is reduced.

NCoR1 overexpression promotes TR α 1 nuclear localization:

Based on our results from the NCoR1 knockdown treatment, we hypothesized that overexpression of NCoR1 would facilitate TR nuclear localization. HeLa cells in the treatment groups were cotransfected with mCherry-TR α 1 and GFP-NCoR1, while the control groups were transfected with only mCherry-TR α 1. The localization patterns of TR α 1 were then analyzed by fluorescence microscopy and N/C ratios were measured. We found that TR α 1 in the control group was mostly localized to the nucleus, while cotransfection of NCoR1 led to an even more robust nuclear localization pattern. There was a significant shift of TR ($p < 0.05$) toward the nucleus in the presence of NCoR1, with an average N/C ratio of 9.5, compared with 8.3 for the control (Figure 4).

The results from NCoR1 shRNA knockdown and NCoR1 overexpression treatment suggested that NCoR1 is one of the factors that contribute to TR's nuclear retention;

there is an increase in TR's nuclear population when NCoR1 is overexpressed and a significant cytosolic shift when NCoR1 is knocked down by shRNA.

AHT-TR α 1 exhibits a significant cytosolic shift:

To further explore TR's interaction with NCoR1, as well as other potential functional implications of mutations within TR's hinge region where NLS-1 resides, we first replicated the studies with the AHT-TR α 1 mutant reported by Baumann et al. [2001]. We transfected HeLa cells with GFP-AHT-TR α 1 (treatment) or wild type GFP-TR α 1 (control). Consistent with the literature, AHT-TR was significantly more cytosolic compared to wild type TR with an average N/C ratio of 3.7, compared with 8.3 for the control ($p < 0.01$) (Figure 5).

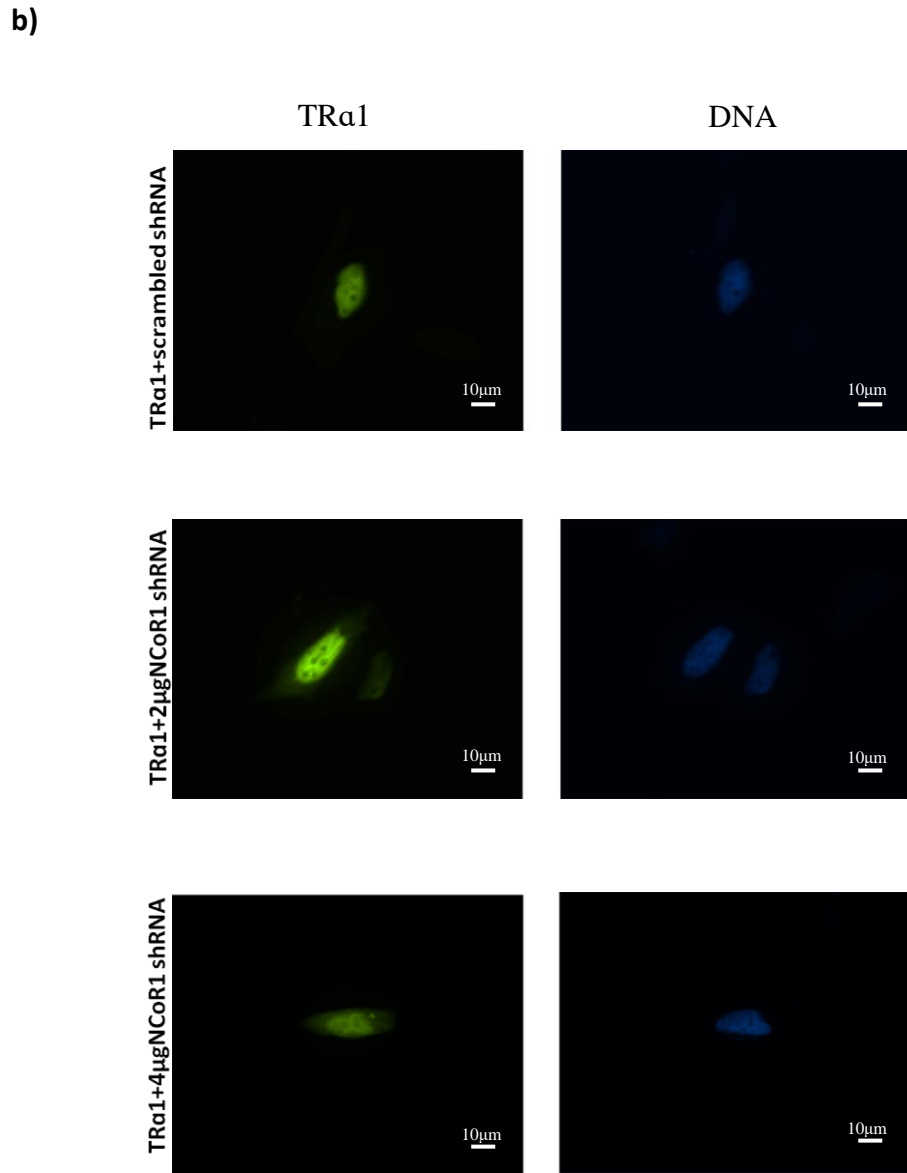
The one dimensional FRAP model could describe the system but modeled molecules tend to diffuse faster:

After identifying the role NCoR1 plays in TR nuclear localization, developing a model that can estimate protein-protein or protein-DNA binding rates was the next goal of this thesis. Because FRAP experiments on cells transfected with both NCoR1 and TR are still in progress (Rochelle Evans, M.S. thesis research), we used our model on previous FRAP data from Mediator 1 (MED1) and TR cotransfection (Femia et al., submitted 2019) to estimate the MED1-TR binding rate. Because we are interested in the protein-protein binding rate, we started by estimating free diffusion of the molecule of interest. Based on the assumption that protein movement can be described with Brownian motion, we first used Stoke Einstein's model to predict the

pure diffusion rate [Einstein, 1905]. Previously, an equation predicting a protein's hybridization radius using its amino acid residues was discovered. Thus, we could apply this equation to calculate the radius of coregulators, TR, and their binding complex [Wilkins et al., 1999]. Using $R_n = (4.75 \pm 1.11)N^{0.29 \pm 0.02}$, we determined that the radius of TR is 29.68Å, the radius of MED1 is 42.04 Å, and their binding complex is 71.72Å. We use this estimated value in the Stoke Einstein's equation [Einstein, 1905], $D = \frac{K_b T}{6\pi\eta r}$, where temperature was set to 310.15 Kelvin (37°C), and viscosity was 0.9mPas[Lippincott-Schwartz et al., 2001; Phair and Misteli, 2000; Kalwarczyk et al., 2011]. We determined that the free diffusion rate for TR is $0.453 \mu m / s^2$, and the diffusion rate for the MED1-TR binding complex is $0.019 \mu m / s^2$. After calculating the pure diffusion parameters, we applied them in the linear FRAP model and numerically fit the model with previous FRAP data for MED1-TR cotransfection experiments [Femia et al., submitted 2019] using Matlab. After fitting the one dimensional FRAP model developed for the linear FRAP method, we obtained a binding rate of $k_{on} = 300$ and $k_{off} = 1$ for the TR-MED1 binding reaction (Figure 6d).

Currently, there exists another FRAP model that is designed for a circular photobleached region. Although the geometry is different from our model, the fluorescent recovery behavior should be similar between the two models. Therefore, it was of interest to observe the predictions of the model. When the diffusion rate and binding rate are constant ($k_{on} = 300, k_{off} = 1$), the two-dimensional model tends to

recover slower due to the extra dimension of movement as shown in Figure 6a. The recovery curve in the circular FRAP model is more sensitive to binding rate change and diffusion rate change, which is shown in Figure 6b and c. Fitting the circular FRAP recovery curve with the MED1-TR data, we obtained a binding rate of $k_{on} = 270$ and $k_{off} = 2$ (Figure 6d). However, due to the difference between the geometry and dimension of the model and that of the experiment, this value does not have any real implication in the system we study, and it is only for model behavior comparison. In the future, it would be necessary to use a circular photobleached region to refit the curve and evaluate the binding rate. One aspect for both models that is worth noticing is that the reaction diffusion equation does not account for fluorescent intensity loss. Therefore, as time goes to infinity, the predicted fluorescent intensity will eventually approach the pre-bleach fluorescent intensity (graph not shown). Therefore, the model requires further modifications in the future.



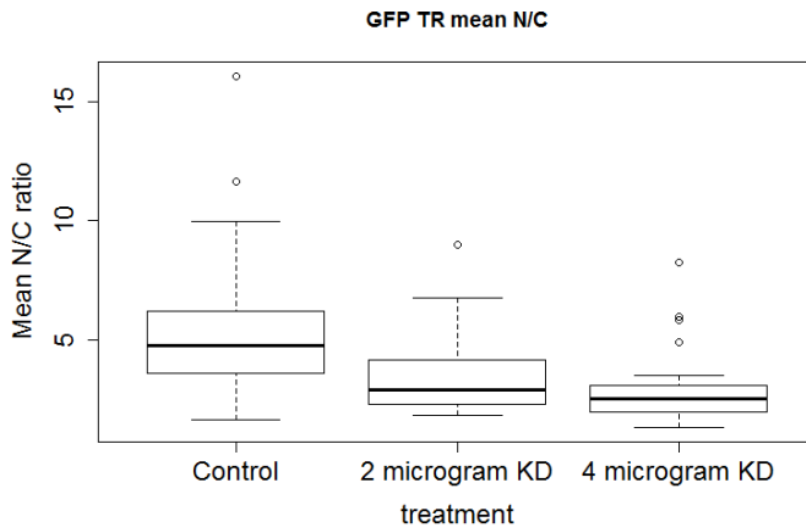


Figure3: NCoR1 knockdown leads to a TR α 1 cytosolic shift. a) HeLa cells were transfected with 4 μ g expression plasmids for NCoR1 shRNA or 4 μ g scrambled shRNA (Control). Western blots of cell lysates were probed with anti-NCoR1 antibody. A decrease in band intensity was observed in the knockdown group, indicating a decrease in levels of endogenous NCoR1. b) HeLa cells were transfected with GFP-TR α 1 and 2 or 4 μ g NCoR1 shRNA. 24 h post transfection, cells were analyzed using fluorescence microscopy. A significant decrease of the N/C ratio was observed in the knockdown group (KD), indicating a greater cytosolic distribution ($p < 0.05$). A higher concentration of transfected shRNA leads to a greater decrease in the N/C ratio (each treatment $n = 100$ with 3 biologically independent replicates)

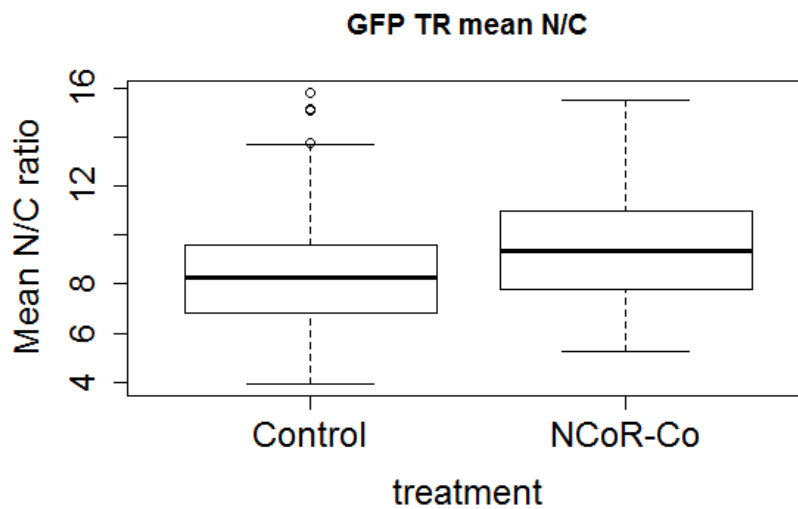
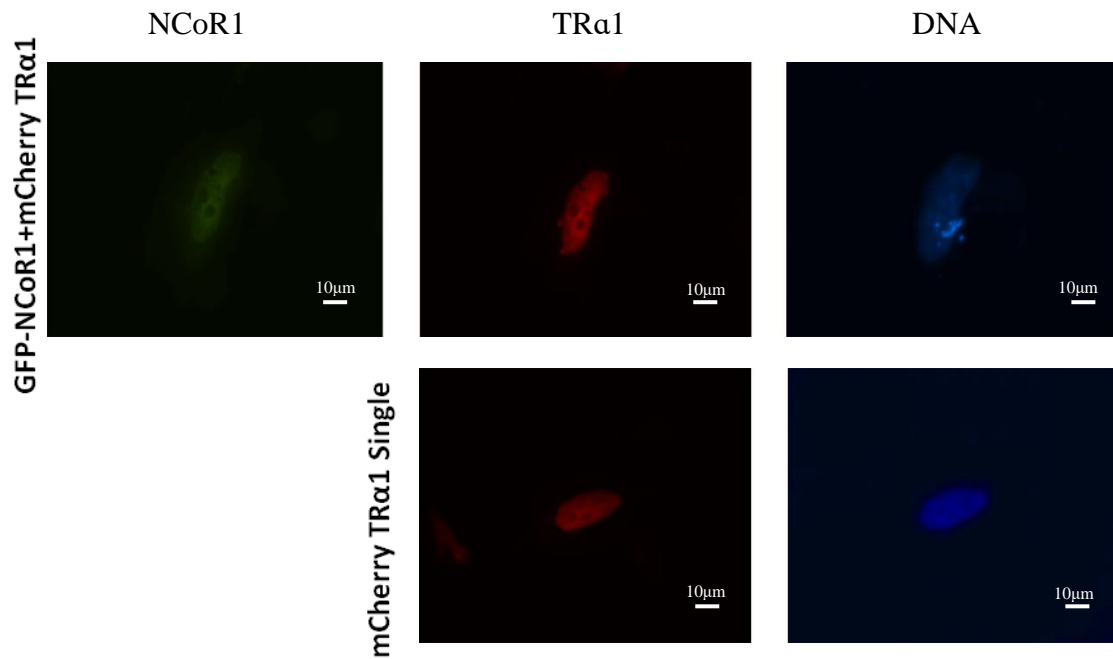


Figure 4: NCoR1 overexpression leads to enhanced TRα1 nuclear localization. HeLa cells were cotransfected with 4μg GFP-NCOR1 and 2μg mCherry-TRα1 or with 2μg mCherry-TRα1. 24 h post transfection, cells were analyzed using fluorescence microscopy. A greater N/C ratio was observed in cells overexpressing NCoR1 (NCoR-Co) compared to the control ($p < 0.05$), indicating that NCoR1 contributes to enhanced TRα1 nuclear retention ($n = 30$ with 10 biologically independent replicates).

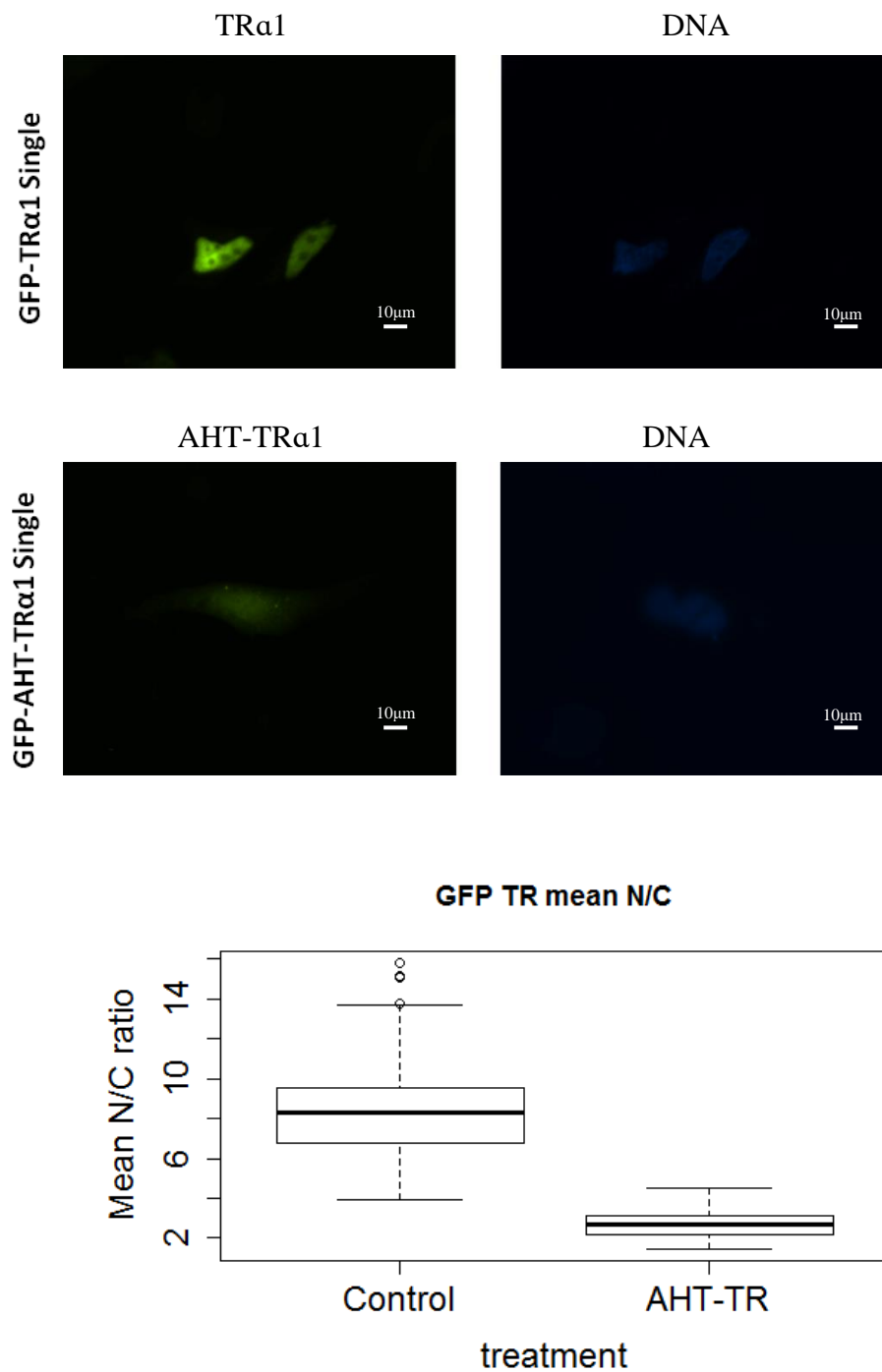
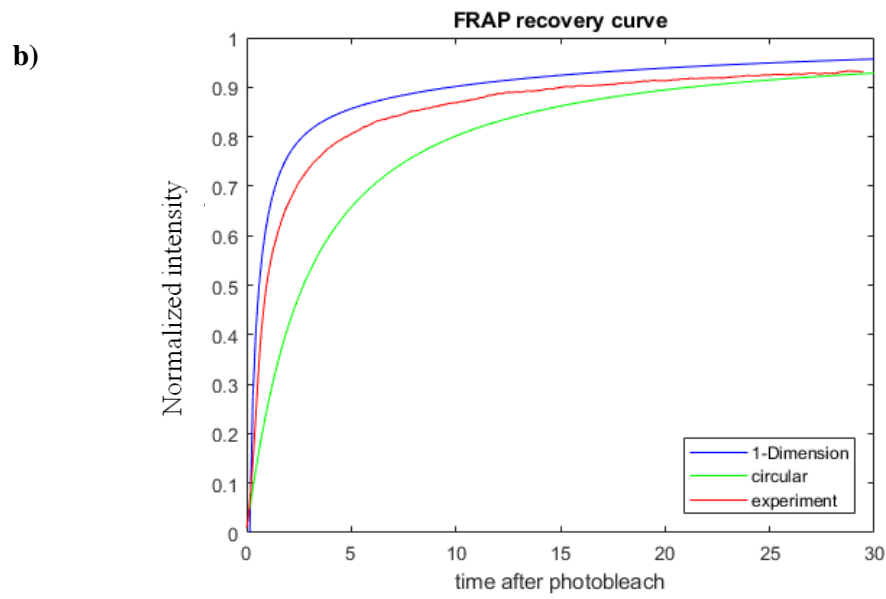
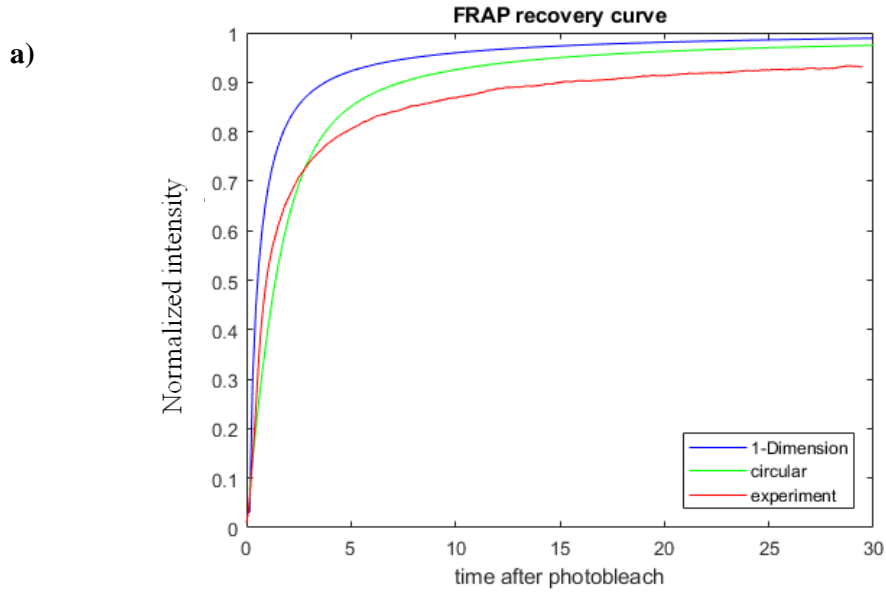


Figure 5: AHT-TR α 1 is more cytosolically distributed compared to wild-type TR α 1. HeLa cells were transfected with 2 μ g GFP-AHT-TR α 1 or 2 μ g GFP-TR α 1. 24 h post transfection, cells were analyzed using fluorescence microscopy. The distribution for AHT mutants was significantly more cytosolic compared to the control group (n=100 with 3 biologically independent replicates).



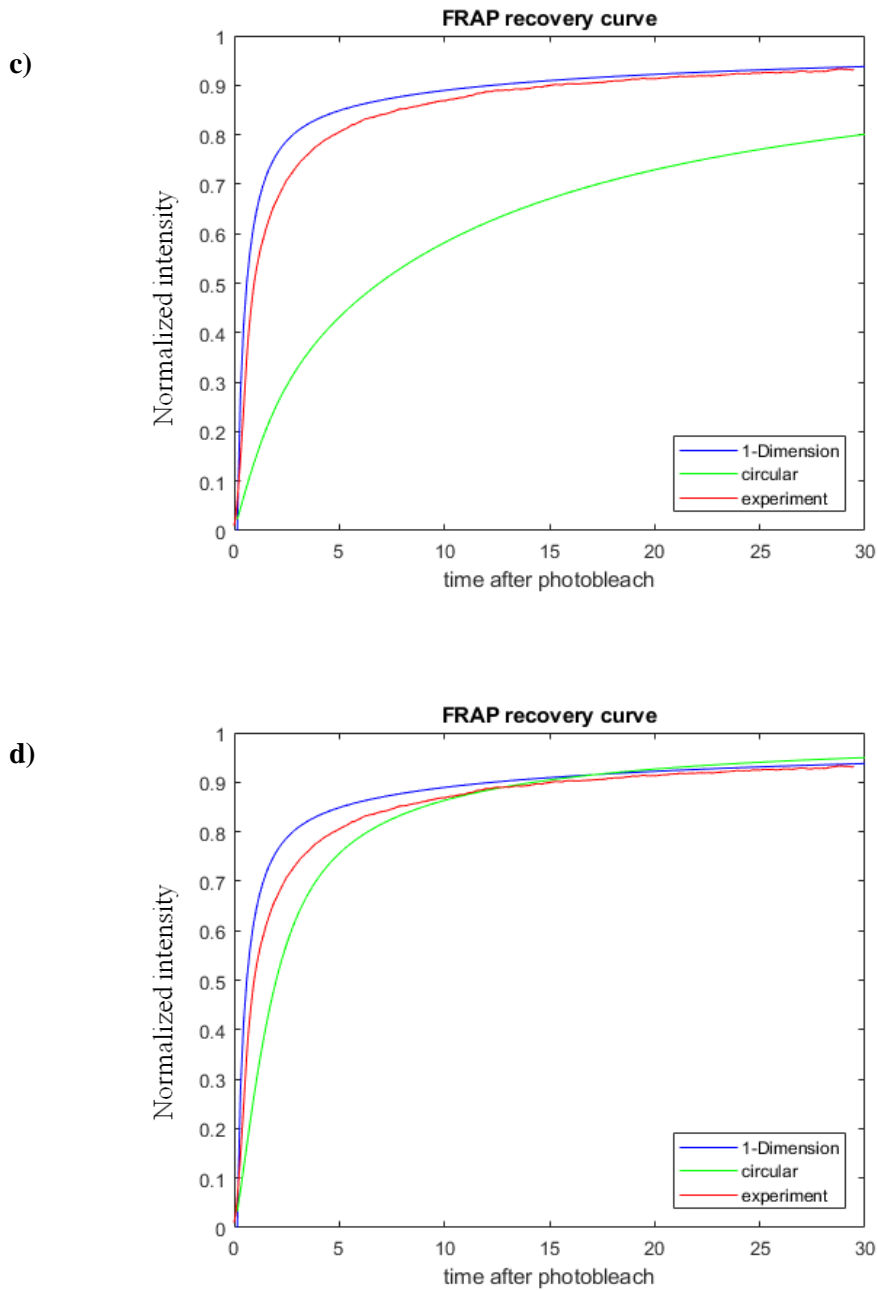


Figure 6: a) As shown in the graph, the 1-dimensional linear FRAP model is blue, 2-dimensional circular FRAP model is green and data from MED1-TR cotransfection is red. When $D_{TR} = 0.45, D_C = 0.019$ and $k_{on} = 30, k_{off} = 1$, the model behavior is similar. However, the predicted recovery is faster in the 1-dimensional model compared to the 2-dimensional model. b) The 2-dimensional circular FRAP model is more sensitive to binding rate change. When diffusion rate is constant, $k_{on} = 200, k_{off} = 1$, there is a bigger change in the curve predicted in the 2-dimensional model. c) The 2-dimensional circular FRAP model is also more sensitive to diffusion rate change. When $D_{TR} = 0.45, D_C = 0.0001$ and $k_{on} = 30, k_{off} = 1$, the model's predicted recovery curve experiences a greater change. d) With settings of $D_{TR} = 0.45, D_C = 0.019$, both models were fit to the data from MED1-TR cotransfection FRAP experiments. For the 1-dimensional line FRAP model, $k_{on} = 300, k_{off} = 1$ and for the 2-dimensional circular FRAP model, $k_{on} = 270, k_{off} = 2$

CHAPTER 4: DISCUSSION

Previous research by Femia et al. [submitted 2019] and Baumann et al. [2001] investigated the effect different coregulators have on TR nuclear retention. These discoveries greatly increase the complexity of TR intracellular dynamics. This thesis research based on Baumann et al.'s hypothesis that NCoR1 is capable of retaining TR in the nucleus, investigated the NCoR1-TR interaction through a different method. Using NCoR1 overexpression and knockdown, we confirmed that NCoR1 contributes to TR nuclear retention. Future experiments on TR β 1 and NCoR1 cotransfection will be of interest. Given TR β 1's slightly more cytosolic population, we predict that the impact of N-CoR1 overexpression on nuclear retention will be even more robust. Furthermore, results from the NCoR1 knockdown experiment imply that TR's nuclear localization is sensitive to the degree of NCoR1 knock down by shRNA. Because the AHT mutant has a mutation in the NCoR1 binding region, its inability to bind to NCoR1 further confirmed the key role that NCoR1 has in TR nuclear retention. As a repression complex, NCoR1's proper binding and release are indispensable for gene transcription initiation. A recent discovery in patients with Resistance to Thyroid Hormone (RTH) syndrome further emphasizes the significance of the NCoR1-TR interaction. This research showed that a TR mutant linked to RTH cannot release NCoR1 in the presence of T₃, leading to cell metabolism disorder [Fozzatti et al., 2011]. Furthermore, study of a truncated NCoR1 homolog that lacks repression ability has strengthened the role NCoR1 has in gene activation and, when misregulated, in thyroid cancer [Fozzatti et al., 2013]. Combined with the discovery of

NCoR1's ability to retain TR in the nucleus, it is possible that NCoR1 controls T3-responsive gene expression both directly through basal transcription regulation and indirectly through maintaining a sufficient nuclear population of TR.

In order to study the intricate TR transport system and eventually model it, the binding rates between TR and different nuclear coregulators must be obtained. This thesis research developed a one-dimensional linear FRAP model that uses a one-dimensional reaction diffusion system to describe the fluorescent recovery curve. Using a reaction diffusion system to describe protein-protein interactions is currently one of the popular methods [Kang et al., 2010]. The system can easily depict the binding interaction between two proteins and provide parameter estimation for the reaction. Compared to a previous existing FRAP model [Kang et al., 2008; Kang et al., 2009], which uses two-dimensional reaction diffusion equations to model the recovery curve, the one-dimensional model we developed is tailored for use with the linear FRAP experiments used in our lab. However, because the linear FRAP model only considers movement of molecules in one dimension, the predicted fluorescent recovery is faster compared to the circular FRAP model. Moreover, the one-dimensional model is less sensitive to parameter change, making it a comparatively less optimal model. In general, the recovery curve has a similar profile when compared to the existing model. The fluorescent molecule will first rapidly exchange with the bleached molecule in the photobleached region. Then, the recovery slows down as the system is closer to equilibrium. The dimension selection sacrifices

some accuracy in recovery rate but allows the system to be generalized and applied to different photobleached areas.

Currently, a model that is capable of describing the competition between multiple protein-protein binding reactions has not been established due to the difficulty of obtaining analytical solutions for high dimension reaction diffusion equations.

Therefore, all the existing FRAP models, including the model presented in this thesis, are based on the assumption that during the FRAP experiment, the reaction between the two co-transfected proteins is dominant and other minor binding interactions can be ignored [Axelrod, 1976; Kang et al., 2008; Kang et al., 2010; Sprague, 2004]. As we identify more TR binding partners in the future, it would be worthwhile to study TR coregulator reactions by biomolecular binding kinetic assays to remove the noise from the system.

The results from various TR mutants discovered in cancer and previous research on AHT-TR clearly indicates that proper localization of TR is essential for normal cell development and function [Bonamy et al., 2005; Zhang et al., 2018]. Therefore, modeling the system of TR shuttling could provide information that is critical for future gene expression models. Previously, a binding competition between MED1 and exportins for TR has been proposed, after MED1 was discovered to contribute to TR nuclear localization [Femia et al., submitted 2019]. Because MED1 binds to the helix 12 region of TR and a NES resides in helix 12 [Savkur and Burris, 2004; Mavinakere et al., 2012; Femia et al., submitted 2019], it is likely that MED1 will block exportins

from binding, allowing TR to remain in the nucleus. Because the binding site of NCoR1 in helix 3 of TR also could conflict with that of exportins, since NES-H3 resides in this region, NCoR1 could then be added to the model to explain the system better [Yen, 2001; Oberoi et al., 2011]. Here, we here proposed a general binding competition model that uses ordinary differential equations to describe the behavior of this system:

$$\begin{aligned}\frac{dTR_c}{dt} &= eTR_N - iTR_c \\ \frac{dN}{dt} &= -k_{on2}NTR_N + k_{off2}C_2 \\ \frac{dM}{dt} &= -k_{on1}MTR_N + k_{off1}C_1 \\ \frac{dTR_N}{dt} &= -eTR_N + iT_c - k_{on1}MTR_N + k_{off1}C_1 - k_{on2}NTR_N + k_{off2}C_2 \\ \frac{dC_1}{dt} &= k_{on1}MTR_N - k_{off1}C_1 \\ \frac{dC_2}{dt} &= k_{on2}NTR_N - k_{off2}C_2\end{aligned}$$

This system currently involves three reactions. First, TR in the nucleus, represented as TR_N , could be exported at rate e to the cytoplasm and become TR_c . The reaction could be reversed by TR nuclear import at rate i . Second, TR_N could bind with MED1, represented as M , to form activation complex C_1 with binding rate k_{on1} . The reaction can be reversed at rate k_{off1} . A similar reaction will happen between TR and NCoR1 at rate k_{on2} and k_{off2} to either form or destroy the repression complex (Figure 7). Once we find reasonable ranges of those parameters, we will be able to study the system's stability and conduct bifurcation analysis. Further, when we give initial values for each variable, we could find the numeric solution for the variable of interest at certain time points and predict TR's localization pattern. The transfection

process is stochastic because different cells will express transfected genes at various levels. Therefore, the ordinary differential equation model could consider including stochasticity to model the *in vitro* experimental outcome better.

In summary, we have observed how NCoR1 affects TRα1 localization using fluorescence microscopy and transient transfection assays. We found that the knockdown of NCoR1 leads to a TRα1 cytosolic shift that is hypothesized to be due to the lack of competitor for exportin binding. An increase in TRα1 nuclear localization was observed when NCoR1 was overexpressed but the increase was modest, due to its original robust nuclear distribution. We have also developed a model that could estimate the binding rate between TR and coregulators which could eventually contribute to a comprehensive TR localization model that we will build in the future.

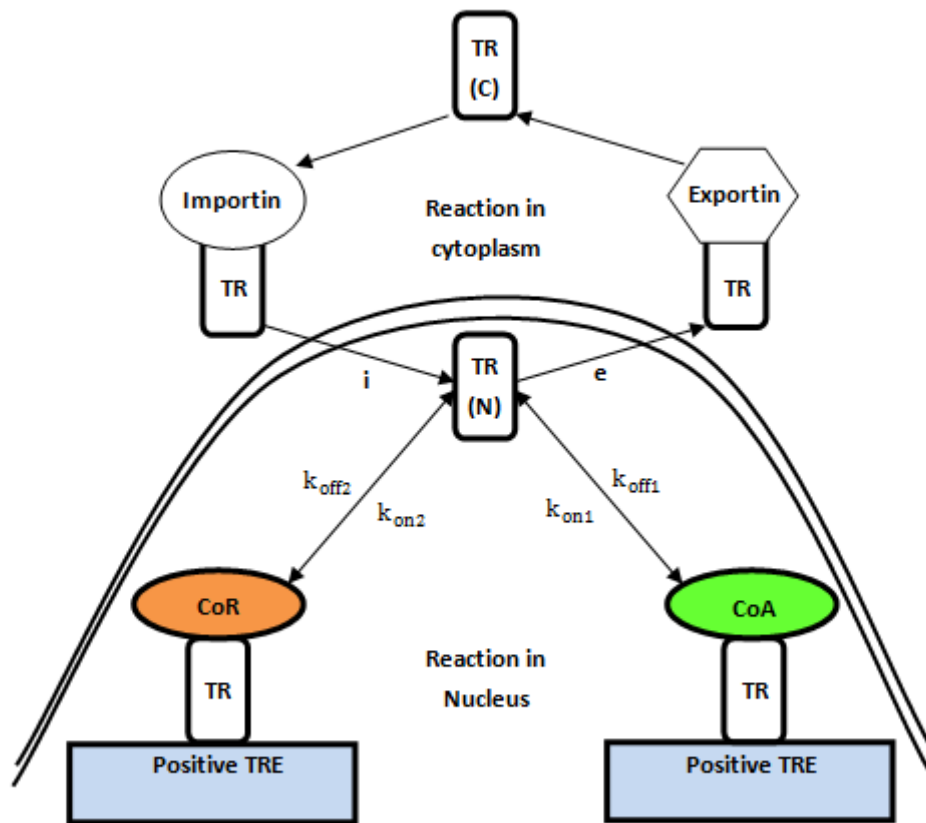


Figure 7: A model for TR localization. The cells are assumed to be provided with a limited amount of ligand. In the nucleus, corepressor NCoR1 and coactivator MED1 will compete for TR binding to either form an activation complex or repression complex. The remainder of the nuclear TR is exported at rate e . The exportin binding process in the nucleus is regarded as irreversible. In the cytoplasm, TR is available for import at rate i , which is also regarded as an irreversible process. In the model, degradation and synthesis are not considered.

Future Directions:

Complete the western blot experiment for NCoR1 knockdown. Because the molecular weight of NCoR1 is over 250 kDa, we must run SDS-PAGE for an extensive amount of time to obtain a good observation of the NCoR1 band. Currently, the lab uses β -tubulin or GAPDH, proteins that exist in all cells, as internal recovery controls and normalization factors; however, as the NCoR1 band reaches the optimal position during SDS-PAGE, β -tubulin and GAPDH have already run off the gel. In the future, we will try three different approaches: 1) improve our western blot protocol and gel run time to allow both β -tubulin or GAPDH and NCoR1 to remain in the gel; 2) find another protein that could be used as a normalization factor with a molecular weight that is high enough to stay in the protein gel as the NCoR1 band reaches the optimal position; 3) use gradient gel on NCoR1 western blot.

Search for other coregulators that contribute to TR nuclear localization. Beyond MED1 and NCoR1, various other coregulators could contribute to TR nuclear retention. Another corepressor, NCoR2 or SMRT, will be a great candidate as it has a similar structure and function as NCoR1. Using knockdown and overexpression, we could observe how the system reacts to the presence of NCoR2. After examining most of the candidates in the system, we could then use statistical analysis on this system to choose the coregulators that affect TR localization the most, while selectively omitting those coregulators that hardly affect the system.

Conduct circular FRAP experiments on MED1-TR and NCoR1-TR system. Although the one-dimensional linear FRAP model could depict the recovery curve, it usually

tends to diffuse faster as it completely ignores movement in two dimensions.

Therefore, it is worthy to repeat the MED1-TR FRAP and NCoR1-TR FRAP using a circular photobleached region and fit the existing two-dimensional circular FRAP model to obtain the parameters. The circular FRAP model can use Gaussian laser profile as initial condition to account for the diffusion that happened before photobleach is complete. Furthermore, we could increase the laser intensity and the radius of the bleached circle so that the recovery can be easier to capture. Using circular FRAP and two-dimensional model could significantly reduce the error from calculations and better depict protein-protein interactions.

Conduct biomolecular binding kinetics assays. Currently, the binding partners for TR in the nucleus have not been completely identified. Therefore, those potential binding partners could affect TR diffusion and eventually stop us from obtaining an accurate binding rate using FRAP. Therefore, performing binding kinetics assays on TR and its known binding partners will help confirm our parameters estimated using FRAP.

Once we understand how much the binding rates from those two methods differ, we could decide which method we should use for future protein-protein binding.

Analyze AHT-TR mutant's binding affinity to other protein. As we understand TR's structure and domains better, we began to question if the AHT mutant that was previously used to study NCoR1-TR localization will interfere with TR's interaction with other coregulators, exportins and importins. Currently, we have tested AHT-TR β 1's binding with importins because TR β 1 only contains one NLS at the

hinge region. The result from coimmunoprecipitation assays and western blotting, however, showed no significant difference in binding compared between the AHT mutant and wild-type TR (data not shown). Recently, GFP-TR α 1 and GFP-TR β 1 mutants with a hinge domain deletion (GFP-TR α 1 Δ hinge and GFP-TR β 1 Δ hinge) were developed. From preliminary transfection experiment, we observed a dramatic shift of GFP-TR α 1 Δ hinge to the cytoplasm. In the future, we plan to test if the hinge-deletion TR mutant still has affinity for importins and coregulators so that they could serve as a negative control for AHT-TR mutants. Furthermore, we could also perform coimmunoprecipitation assays and western blotting on other known partners that bind to TR's hinge region to determine if the mutation has any effect on those binding partners. Meanwhile, the lab is working on protein structure predictions on various mutants. Therefore, we could use existing models to predict the structure of AHT-TR and predict its interaction with other proteins using this model.

TR nuclear export and import rate calculation. In the model presented in the discussion section, export rate and import rate are the other two significant parameters. The nuclear shuttling system can be described with an ODE system; however, we must remove all the interfering binding partners if we would like to increase the accuracy of the parameter estimation. Currently, more research and literature review are required before we could solve this problem. Once the range of the nuclear export and import rate is obtained, we could apply these values along with the binding rate to

the TR localization model. The model could help us analyze the system's stability and predict the system's behavior when the parameters change.

Reference:

1. Aifantis, E., and J. Hill. (1980) On the theory of diffusion in media with double diffusivity. I. Basic mathematical results. *Q. J. Mech. Appl. Math.* 33:1–21.
2. Axelrod, D., D. Koppel, J. Schlessinger, E. Elson, and W. Webb. (1976) Mobility measurement by analysis of fluorescence photobleaching recovery kinetics. *Biophys. J.* 16:1055–1106.
3. Baumann CT, Maruvada P, Hager GL, Yen PM. (1980) Nuclear cytoplasmic shuttling by thyroid hormone receptors. multiple protein interactions are required for nuclear retention. *J Biol Chem.* 276(14):11237–11245.
4. Bonamy G. M., Guiochon-Mantel A., Allison L. A. (2005) Cancer promoted by the oncoprotein v-ErbA may be due to subcellular mislocalization of nuclear receptors. *Mol Endocrinol*19:1213–30.
5. Bunn, C.F., Neidig, J.A., Freidinger, K.E., Stankiewicz, T.A., Weaver, B.S., McGrew, J., Allison, L.A. (2001) Nucleocytoplasmic shuttling of the thyroid hormone receptor alpha. *Molecular Endocrinology* 15: 512-533.
6. Brangwynne CP, Koenderink GH, MacKintosh FC, Weitz DA. (2008) Cytoplasmic diffusion: molecular motors mix it up. *J Cell Biol* 183: 583–587.
7. Brent GA. (2012) Mechanisms of thyroid hormone action. *J Clin Invest*122: 3035–3043.
8. Anyeteyi, C.A., Roggero, V.R., Allison, L.A. (2018) Thyroid hormone receptor localization in target tissues. *Journal of Endocrinology*, 237, R19-R34.
9. Davis P. J., Lin H. Y., Mousa S. A., Luidens M. K., Hercbergs A. A., Wehling M., et al. (2011) Overlapping nongenomic and genomic actions of thyroid hormone andsteroids. *Steroids* 76: 829–833.
10. Duma D., Jewell C.M., Cidlowski J.A. (2006) Multiple glucocorticoid receptor isoforms and mechanisms of post-translational modification. *J. Steroid Biochem. Mol. Biol*102: 11–21
11. Einstein A. (1905) On the electrodynamics of moving bodies *Ann. Phys*17: 891
12. Elbashir S.M., Lendeckel,W. and Tuschl,T. (2001b) RNA interference is mediated by 21 and 22 nt RNAs. *Genes Dev* 15: 188–200.
13. Fire A., Xu S., Montgomery M.K., Kostas S.A., Driver S.E., Mello C.C. (1998) Potent and specific genetic interference by double-stranded RNA in caenorhabditis elegans. *Nature*391: 806–811.
14. Fozzatti L., Lu C., Kim D.W., Park J.W., Astapova I., Gavrilova O., Willingham M.C., Hollenberg A.N., Cheng S.Y. (2011) Resistance to thyroid hormone is modulated in vivo by the nuclear receptor corepressor (NCOR1) *Proc. Natl. Acad. Sci. U. S. A*108: 17462–17467.
15. Fozzatti L., Kim D.W., Park J.W., Willingham M.C., Hollenberg A.N., Cheng S.Y. (2013) Nuclear receptor corepressor (NCOR1) regulates in vivo actions of a mutated thyroid hormone receptor α *Proc. Natl. Acad. Sci. U. S. A*110: 7850–7855.
16. Fischle W., Dequiedt F, Hendzel M.J., Guenther M.G., Lazar M.A., Voelter W., Verdin E. (2002) Enzymatic activity associated with class II HDACs is dependent on a multiprotein complex containing HDAC3 and SMRT/N-CoR. *Mol. Cell*9: 45–57.

-
17. Gnocchi D, Steffensen KR, Bruscalupi G, Parini P. (2016) Emerging role of thyroid hormone metabolites. *Acta Physiol* 217: 184–216
 18. García-Silva S, Martínez-Iglesias O, Ruiz-Llorente L, Aranda A. (2011) Thyroid hormone receptor β 1 domains responsible for the antagonism with the ras oncogene: role of corepressors. *Oncogene*30: 854–864.
 19. Görlich D., Vogel F., Mills A.D., Hartmann E., Laskey R.A. (1995) Distinct functions for the two importin subunits in nuclear protein import. *Nature*377: 246–248.
 20. Görlich D., Panté N., Kutay U., Aebi U., Bischoff F.R. (1996) Identification of different roles for RanGDP and RanGTP in nuclear protein import. *EMBO J*15 :5584–5594.
 21. Heinzl T, Lavinsky RM, Mullen TM, Söderstrom M, Laherty CD, Torchia J, Yang WM, Brard G, Ngo SD, Davie JR, et al. (1997). A complex containing N-CoR, mSin3 and histone deacetylase mediates transcriptional repression. *Nature* 387: 43–48.
 22. Hoelz A, Debler EW, Blobel G. (2011) The structure of the nuclear pore complex. *Annu Rev Biochem*80:613 - 643.
 23. Horlein AJ, Naar AM, Heinzl T, Torchia J, Gloss B, Kurokawa R. et al. (1995) Ligand-independent repression by the thyroid hormone receptor mediated by a nuclear receptor co-repressor. *Nature*377: 397–404.
 24. Hudson G.M., Watson P.J., Fairall L., Jamieson A.G., Schwabe J.W. (2015) Insights into the recruitment of class IIa histone deacetylases (HDACs) to the SMRT/NCoR transcriptional repression complex. *J. Biol. Chem*290: 18237–18244.
 25. Jazdzewski K, Boguslawska J, Jendrzewski J, Liyanarachchi S, Pachucki J, Wardyn KA, Nauman A, de la Chapelle A. (2011) Thyroid hormone receptor β (THRB) is a major target gene for microRNAs deregulated in papillary thyroid carcinoma (PTC). *J Clin Endocrinol Metab* 96:E546–E553
 26. Johnson, BA, Wilson, EM, Li, Y, Moller, DE, Smith, RG, Zhou, G (2000) Ligand - induced stabilization of PPARgamma monitored by NMR spectroscopy: implications for nuclear receptor activation. *J Mol Biol* 298: 187– 194.
 27. Kalwarczyk T, et al (2011). Comparative analysis of viscosity of complex liquids and cytoplasm of mammalian cells at the nanoscale. *Nano Lett*11:2157–2163.
 28. Kang M., Kenworthy A.K. (2008) A closed-form analytic expression for FRAP formula for the binding diffusion model. *Biophys. J*95:L13–L15
 29. Kang M., Day C.A., DiBenedetto E. (2009) A generalization of theory for two-dimensional fluorescence recovery after photobleaching applicable to confocal laser scanning microscopes. *Biophys. J*97:1501–1511.
 30. Kang M, Day CA, Di Benedetto E, Kenworthy AK. (2010) A quantitative approach to analyze binding diffusion kinetics by confocal FRAP. *Biophys. J*99:2737–2747.
 31. Kim HJ, Balczak TJ, Nathin SJ, McMullen HF, Hansen DE. (1992) The use of a spectrophotometric assay to study the interaction of S-adenosylmethionine synthetase with methionine analogues. *Anal Biochem*207(1):68–72.
 32. Lippincott-Schwartz J, Snapp E, Kenworthy A. (2001) Studying protein dynamics in living cells. *Nat. Rev. Mol. Cell Biol*2:444–456.

-
33. Nagy L., Kao H.Y., Love J.D., Li C., Banayo E., Gooch J.T., Krishna V., Chatterjee K., Evans R.M., Schwabe J.W. (1999) Mechanism of corepressor binding and release from nuclear hormone receptors. *Genes Dev*13:3209–3216.
34. Makowski A, Brzostek S, Cohen RN, Hollenberg AN. (2003) Determination of nuclear receptor corepressor interactions with the thyroid hormone receptor. *Mol Endocrinol*17:273–286.
35. Maniataki E, Mourelatos Z. (2005) A human, ATP-independent, RISC assembly machine fueled by pre-miRNA. *Genes & Dev*19:2979–2990.
36. Marsili A., Tang D., Harney J.W., Singh P., Zavacki A.M., Dentice M., Salvatore D., Larsen P.R. (2011) Type II iodothyronine deiodinase provides intracellular 3,5,3'-triiodothyronine to normal and regenerating mouse skeletal muscle. *Am. J. Physiol. Endocrinol. Metab*301:E818–E824.
37. Mavinakere MS, Powers JM, Subramanian KS, Roggero VR, Allison LA. (2012) Multiple novel signals mediate thyroid hormone receptor nuclear import and export. *J Biol Chem*287:31280–31297.
38. Moore CB, Guthrie EH, Huang MTH, Taxman DJ. (2010) Short hairpin RNA (shRNA): design, delivery, and assessment of gene knockdown. *Methods Mol. Biol*629:141–158.
39. Oberoi J., Fairall L., Watson P.J., Yang J.-C., Czimmerer Z., Kampmann T., Goult B.T., Greenwood J.A., Gooch J.T., Kallenberger B.C. (2011) Structural basis for the assembly of the SMRT/NCOR core transcriptional repression machinery. *Nat. Struct. Mol. Biol*18:177–184.
40. Pemberton L. F., Paschal B. M. (2005). Mechanisms of receptor-mediated nuclear import and nuclear export. *Traffic* 6, 187–198.
41. Perissi V, et al. (1999) Molecular determinants of nuclear receptor-corepressor interaction. *Genes Dev*13:3198–3208.
42. Phair RD, Misteli T. (2000) High mobility of proteins in the mammalian cell nucleus. *Nature*404:604–609.
43. Pissios, P, Tzamelis, I, Kushner, P, Moore, DD (2000) Dynamic stabilization of nuclear receptor ligand binding domains by hormone or corepressor binding. *Mol Cell* 6: 245– 253.
44. Roggero, V.R., Zhang, J., Parente, L.E., Doshi, Y., Dziedzic, R.C., McGregor, E.L., Varjabedian, A.D., Schad, S.E., Bondzi, C., Allison, L.A. (2016) Nuclear import of the thyroid hormone receptor alpha1 is mediated by importin 7, importin beta1, and adaptor importin alpha1. *Molecular and Cellular Endocrinology* 419: 185-197.
45. Roosen-Runge F, et al. (2011) Protein self-diffusion in crowded solutions. *Proc. Natl. Acad. Sci. USA*108:11815–11820.
46. Savkur R.S., Burris T.P. (2004) The coactivator LXXLL nuclear receptor recognition motif. *J. Pept. Res*63:207–212.
47. Seiffers S, Oppermann W. (2005) Systematic evaluation of FRAP experiments performed in a confocal laser scanning microscope. *J Microsc*220(1):20–30.
48. Selmi-Ruby S, Rousset B. (1996) Analysis of the functional state of T3 nuclear receptors expressed in thyroid cells. *Mol Cell Endocrinol*119(1):95–104.

-
49. Selmi-Ruby S, Casanova J, Malhotra S, Roussett B, Raaka BM, Samuels HH. (1998) Role of the conserved C-terminal region of thyroid hormone receptor-alpha in ligand-dependent transcriptional activation. *Molecular and cellular endocrinology*138(1-2):105–114.
50. Sorokin AV, Kim ER, Ovchinnikov LP. (2007) Nucleocytoplasmic transport of proteins. *BiochemBiokhimiia*72:1439–1457.
51. Sprague BL, Pego RL, Stavreva DA, McNally JG. (2004) Analysis of binding reactions by fluorescence recovery after photobleaching. *Biophys. J*86:3473–95.
52. Subramanian KS, Dziedzic RC, Nelson HN, Stern ME, Roggero VR, Bondzi C, Allison LA. (2015) Multiple exportins influence thyroid hormone receptor localization. *Mol Cell Endocrinol*411:86–96.
53. Suntharalingam M, Wenthe SR. (2003) Peering through the pore: nuclear pore complex structure, assembly, and function. *Dev. Cell*4:775–789.
54. Vandevyver S., Dejager L., Libert C. (2012). On the trail of the glucocorticoid receptor: into the nucleus and back. *Traffic* 13, 364–374
55. Wagner RL, Apriletti JW, McGrath ME, West BL, Baxter JD, Fletterick RJ. (1995) A structural role for hormone in the thyroid hormone receptor. *Nature*378:690–697.
56. Watson P.J., Fairall L., Santos G.M., Schwabe J.W.R. (2012) Structure of HDAC3 bound to co-repressor and inositol tetrakisphosphate. *Nature*481:335–340.
57. Weikum ER, Liu X, Ortlund EA. (2018) The nuclear receptor superfamily: A structural perspective. *Protein Sci.*27(11):1876-1892.
58. Wilkins DK, Grimshaw SB, Dobson CM, Jones JA, Smith LJ. (1999) Hydrodynamic radii of native and denatured proteins measured by pulse field gradient NMR techniques. *Biochemistry*38:16424–16431.
59. Yen PM. (2001) Physiological and molecular basis of thyroid hormone action. *Physiol Rev*81:1097–142.
60. Yen PM, Ando S, Feng X, Liu Y, Maruvada P, Xia X. (2006) Thyroid hormone action at the cellular, genomic and target gene levels. *Mol Cell Endocrinol*246:121–7.
61. Zhang J., Lazar M. A. (2000) The mechanism of action of thyroid hormones. *Annual Review of Physiology*62(1):439–466.
62. Zhang, J., Roggero, V.R., Allison, L.A. (2017) Nuclear import and export of the thyroid hormone receptor. Chapter 3 in *Thyroid Hormone*, G. Littwack, ed., *Vitamins and Hormones* 106, 45-66.